CHINESE OPTICS LETTERS

Vol. 21, No. 1 | January 2023

Vibration measurement with frequency modulation single-pixel imaging

Wenxin Zhang (章文欣)[1,2*], Yuxiu Tao (陶钰秀)[1], Yangkang Wu (吴杨康)[1], Fu Zhu (祝 福)[1], Wenchao Cai (蔡文超)[1], Ning Liu (刘 宁)[1], Qiang Zhao (赵 强)[1], and Ping Xue (薛 平)[2]

[1] College of Electronic and Optical Engineering & College of Flexible Electronics (Future Technology), Nanjing University of Posts and Telecommunications, Nanjing 210023, China

[2] State Key Laboratory of Low-Dimensional Quantum Physics and Department of Physics, Collaborative Innovation Center of Quantum Matter, Tsinghua University, Beijing 100084, China

*Corresponding author: zhangwx@njupt.edu.cn

Received June 15, 2022 | Accepted August 10, 2022 | Posted Online September 7, 2022

Single-pixel imaging can reconstruct the image of the object when the light traveling from the object to the detector is scattered or distorted. Most single-pixel imaging methods only obtain distribution of transmittance or reflectivity of the object. Some methods can obtain extra information, such as color and polarization information. However, there is no method that can get the vibration information when the object is vibrating during the measurement. Vibration information is very important, because unexpected vibration often means the occurrence of abnormal conditions. In this Letter, we introduce a method to obtain vibration information with the frequency modulation single-pixel imaging method. This method uses a light source with a special pattern to illuminate the object and analyzes the frequency of the total light intensity signal transmitted or reflected by the object. Compared to other single-pixel imaging methods, frequency modulation single-pixel imaging can obtain vibration information and maintain high signal-to-noise ratio and has potential on finding out hidden facilities under construction or instruments in work.

Keywords: single-pixel imaging; frequency modulation; vibration measurement.

DOI: 10.3788/COL202321.011102

1. Introduction

Single-pixel imaging can reconstruct the 2D image of the object when the light traveling from the object to the detector is scattered or distorted, so it is widely used in some complicated situations, such as in smoke, turbulence, or water where other optical methods cannot implement imaging. It has huge potential in defense and civil and has became a research hotspot in the field of optical imaging recently. Single-pixel imaging is often referred to ghost imaging[1], especially computational ghost imaging[2], because both of them illuminate the object with light patterns and use a single-pixel detector to detect the scattered light from the object[3]. At first, ghost imaging was more popular, but it has the problem of extremely low imaging signal-to-noise ratio (SNR)[4]. Compared to computational ghost imaging, where the light patterns are random, single-pixel imaging usually has better SNR by designing the light patterns carefully[5].

Several methods were developed to improve the SNR of single-pixel imaging and ghost imaging, such as differential ghost imaging[6], iterative algorithm[7,8], Gerchberg–Saxton-like single-pixel image[9], and imaging of a reflective object using positive and negative correlations[10]. Compared to the methods above, single-pixel imaging that used special light patterns has obvious advantages in SNR, for example, the compressive sensing computational single-pixel imaging method[11,12], Fourier spectrum retrieval method[13], and Fourier spectrum acquisition method[3]. All these methods greatly improve the SNR and make single-pixel imaging more suitable for use.

Some methods can obtain extra information. The colored object encoding scheme was used in single-pixel imaging systems to get the color of the object[14], and the polarimetric single-pixel imaging method can be used to obtain polarization information[15]. However, we still cannot get the vibration information when the object is vibrating during the measurement, and the single-pixel image will also blur.

2. Theory

In this Letter, we use a method called frequency modulation single-pixel imaging (FMSI) to detect the vibration of the object. FMSI uses a light source with a special pattern to illuminate the object, which can ensure that the light intensity signals at different positions have different frequencies. When the object is vibrating, there will be an extra intensity modulation on the light, and the frequency of the position will be changed. By analyzing the change of the frequency, we can obtain the information of the position and frequency of the vibration. By getting the vibration information, FMSI has the potential to finding abnormal conditions such as hidden facilities under construction or unexpected instruments in work.

The optical design of FMSI is shown in Fig. 1. An LED array is used as a light source to illuminate the object. The distance between the objects and LED array is 2 cm, and the distance between the objects and sensor is about 40 cm. The pattern of the LED is well designed, and the light pattern on the sample is almost the same as the LED pattern because the distance between the object and sample is quite small. If the distance becomes large, the lights from different LEDs will mix with each other, and the final image will blur. The image we finally obtain is the convolution of the pattern of the object and point spread function (PSF), which can be obtained by the light intensity distribution function on the object of a single superluminescent diode (SLD). In this circumstance, a lens can be placed between the light source and object to project the pattern of the light source onto the object to reduce PSF. The light pattern on the sample has sequence intensity distribution $I(x,y,n)$. n represents the series number of the light pattern, and (x,y) represents the position of the object.

As the objects have different transmittance, part of the light passes through the object and finally enters the power sensor. As single-pixel imaging is usually used in complicated situations where there are obstacles or distortions which will disturb the light from the object between the detector and the object, a piece of ground glass is placed before the detector as a barrier to distort the light. Of course, we can still obtain the image without the ground glass, and the image will be even better because the power sensor receives more light. S_n is the sequence signal detected by the power sensor.

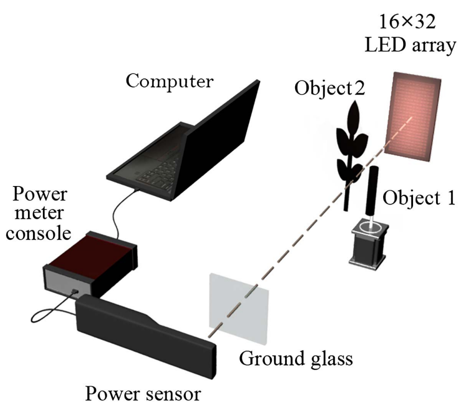

Fig. 1. Optical design of FMSI. The light-emitting diode (LED) array is 32 × 16 pixels, and each pixel is 5 mm × 5 mm. Power sensor: S130C, Thorlabs; power meter console: PM100USB, Thorlabs.

When the sequence light intensity pattern $I(x,y,n)$ is random, the light intensity signals at different positions are not orthogonal to each other. That results in the quite low SNR in the traditional algorithm. Also, we cannot get the vibration information in this circumstance.

In order to distinguish information from different positions and get the vibration information, we should make the sequence light intensity signals at different positions orthogonal to each other. As the trigonometric function is one of the most commonly used and most compact orthogonal functions, we use it to modulate the light. We make the light intensity signals at different positions have different frequencies, and the light intensity distribution at position (x,y) can be expressed as

$$I(x,y,n)=\{1+\cos[\pi(Xy+x-X)n/XY]\}/2;\quad x\in[1,X],\quad y\in[1,Y],\quad n\in[1,2XY]. \tag{1}$$

The light then passes through the object and ground glass and reaches the detector. The signal at the detector is

$$\begin{aligned}S(n)&=\sum t(x,y)\times I(x,y,n)\\&=\sum t(x,y)\times\{1+\cos[\pi(Xy+x-X)n/XY]\}/2,\end{aligned} \tag{2}$$

where $t(x,y)$ represents the transmittance of the object at the position (x,y).

From Eq. (2), we can see that when the object is stable, the sequence signal at the detector is the sum of a constant and the cosine transformation of the transmittance distribution function $t(x,y)$ of the object. So, the transmittance distribution function $t(x,y)$ can be obtained by the cosine transformation of the signal,

$$\begin{aligned}t'(p)&=\sum_n S(n)\cos(2\pi pn/2XY)\\&=\sum_n\sum_{x,y}t(x,y)\times\{1+\cos[\pi(Xy+x-X)n/XY]\}/2\\&\quad\times\cos(\pi pn/XY)\\&\propto\sum_{x,y}t(x,y)\delta(p=Xy+x-X)+\text{const}.\end{aligned} \tag{3}$$

When the object is vibrating, as long as there is a vibration component perpendicular to the propagation direction of the light, the transmittance at the edge of the object will change with time.

The transmittance at the edge of the object can be written as

$$t(x_v,y_v,t)=t(x_v,y_v)\times[1+A\cos(2\pi ft+\phi)]/2. \tag{4}$$

The sequence signal at the detector will also be changed,

$$\begin{aligned} S(n) &= \sum t(x,y)\times I(x,y,n)\\ &= \sum_{x_s,y_s} t(x_s,y_s)\times\{1+\cos[\pi(Xy_s+x_s-X)n/XY]\}/2\\ &\quad+\sum_{x_v,y_v} t(x_v,y_v,t)\times\{1+\cos[\pi(Xy_v+x_v-X)n/XY]\}/2\\ &= \sum_{x_s,y_s} t(x_s,y_s)\times\{1+\cos[\pi(Xy_s+x_s-X)n/XY]\}/2\\ &\quad+\sum_{x_v,y_v} t(x_v,y_v)\times[1+A\cos(2\pi ft+\phi)]/2\\ &\quad\times\{1+\cos[\pi(Xy_v+x_v-X)n/XY]\}/2, \end{aligned} \tag{5}$$

where (x_s, y_s) represents the position where the object is stable or the position in the vibrating object, where the transmittance does not change. (x_v, y_v) represents the position at the edge of the vibrating object where the transmittance is changing with time. Furthermore, the transmittance at (x_v, y_v) changes at the same frequency f with the vibrating of the object. Φ is a constant that represents the initial phase, A is a constant that represents the amplitude of the vibration, and $A \in [0, 1]$. Here, we assume that the amplitude of the vibration is less than the size of one pixel.

By doing cosine transformation of the signal $S(n)$, the information of the transmittance distribution and the frequency of the vibration can be obtained,

$$\begin{aligned} t'(p) &= \sum_n S(n)\cos(2\pi pn/2XY)\\ &= \sum_n\sum_{x_s,y_s} t(x_s,y_s)\times\{1+\cos[\pi(Xy_s+x_s-X)n/XY]\}/2\\ &\quad\times\cos(\pi pn/XY)\\ &\quad+\sum_n\sum_{x_v,y_v}\{t(x_v,y_v)\times[1+A\cos(2\pi ft+\phi)]/2\\ &\quad\times\{1+\cos[\pi(Xy_v+x_v-X)n/XY]\}/2\}\times\cos(\pi pn/XY)\\ &\propto \sum_{x_s,y_s} t(x_s,y_s)\delta(p=Xy_s+x_s-X)/2+\text{const1}\\ &\quad+\text{const2}+\sum_{x_v,y_v}[At(x_v,y_v)\delta(p=2fXYt/n)]/4\\ &\quad+\sum_{x_v,y_v}[t(x_v,y_v)\delta(p=Xy_v+x_v-X)]/4\\ &\quad+\sum_{x_v,y_v} At(x_v,y_v)\delta[p=2fXYt/n+(Xy_v+x_v-X)]/8\\ &\quad+\sum_{x_v,y_v} At(x_v,y_v)\delta[p=2fXYt/n-(Xy_v+x_v-X)]/8, \end{aligned} \tag{6}$$

where const1 and const2 are two constants that appear at $p = 0$ and have little effect on our result. From Eq. (6), we can see that the signal $t'(p)$ contains three parts:

A: at the area where the transmittance is constant, the result is the same as Eq. (3),

$$t(x_s,y_s)\propto t'(p),\qquad p=Xy+x-X; \tag{7}$$

B: a signal will appear at the vibration frequency,

$$p=2fXYt/n=fT,\qquad \text{where } T \text{ is the measurement time, frequency of the light pattern is } n/t=2XY/T; \tag{8}$$

C: the signal of the edge of the object where the transmittance is oscillating with time will appear at three frequencies,

$$\begin{aligned} t'(p) &\propto \sum_{x_v,y_v}[t(x_v,y_v)\delta(p=Xy_v+x_v-X)]/4\\ &\quad+\sum_{x_v,y_v} At(x_v,y_v)\delta[p=2fXYt/n+(Xy_v+x_v-X)]/8\\ &\quad+\sum_{x_v,y_v} At(x_v,y_v)\delta[p=2fXYt/n-(Xy_v+x_v-X)]/8. \end{aligned} \tag{9}$$

The first term appears at the same position when the object is stable. The second and third terms distribute symmetrically on both sides of the vibration frequency.

In order to avoid the signals overlapping with each other, the position of the vibration signal with smaller frequency should be larger than that of the signal of the stable object. So, we should have

$$f-(Xy_v+x_v-X)/T > XY/T. \tag{10}$$

3. Simulation

The simulations of the vibration measurement with FMSI are shown in Fig. 2. When all the objects are stable, FMSI can retrieve the image perfectly, as shown in Figs. 2(b) and 2(c). When object 1 is vibrating, the edge of the object will blur, as shown in Fig. 2(e), a signal appears at the vibration frequency, and the signal of the edge of the object appears at both sides of the vibration signal, as shown in Fig. 2(e). In Fig. 2(f), the position of the vibrating object can be found by the edge of the object.

In fact, the amplitude of the vibration may not be less than the size of one pixel. If the amplitude is larger than one pixel, the frequency distribution of the transmittance will change.

Simulations when the amplitude of the vibration is larger than one pixel are shown in Fig. 3. When the amplitude is 1.6 times the length of the pixel and the edge of the object is vibrating between pixel 1 and pixel 2, the transmittance of each pixel is shown in Figs. 3(b) and 3(c). By Fourier transformation, we can see that the harmonics appear. Fortunately, the frequency of the vibration is the same as the base frequency, and the signal of harmonics and the vibration object will not overlap with each other due to Eq. (10).

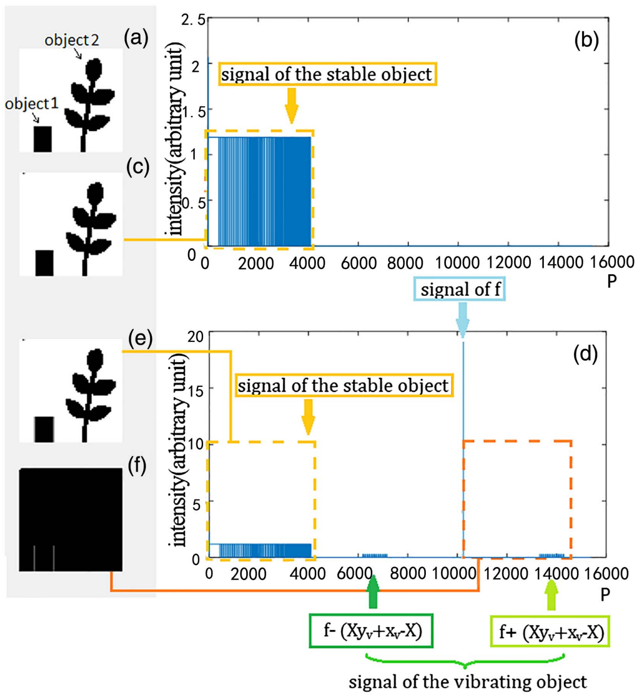

Fig. 2. Simulations of the vibration measurement with FMSI. (a) The original binary sample (64×64), (b) Fourier transformation of the signal when all the objects are stable, (c) single-pixel image when all the objects are stable, (d) Fourier transformation of the signal when object 1 is vibrating horizontally, (e) single-pixel image when object 1 is vibrating horizontally, and (f) single-pixel image of vibrating area.

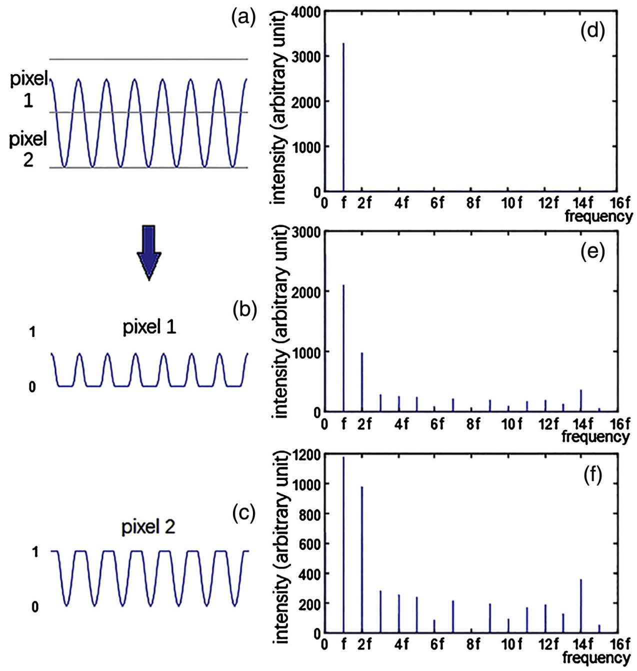

Fig. 3. Frequency distribution of transmittance when the amplitude of the vibration is larger than one pixel. (a) The edge of the object vibrating between pixel 1 and pixel 2. Pixel 1 and pixel 2 are the two pixels affected by the vibration edge, where the amplitude of the vibration is 1.6 times the length of the pixel. (b) and (c) Change of transmittance at the pixel 1 and pixel 2, (d) frequency of the vibration, (e) and (f) frequency of transmittance of pixel 1 and pixel 2.

4. Experiment

A stable leaf and a vibrating cylinder are used as samples to further experimentally verify the feasibility of FMSI to measure vibration. We use a 32×16 pixels light source and measure its transmittance. The optical design is the same as Fig. 1. A stepper motor is used to drive the cylinder to rotate eccentrically, so there is a vibration component perpendicular to the propagation direction of the light. In our experiment, we set the rotating speed so the frequency of the vibration component can be determined. We then use our method to detect the position and frequency of the vibration.

The experiment results of single-pixel imaging are shown in Figs. 4 and 5. The Nyquist sampling rule requires twice the highest frequency of the signal of sample. If all the object is stable, the highest frequency from the object is XY/T, so the sample frequency and the frequency of the light pattern are $2XY/T$, as in Eq. (2). The mirror image will appear at $p \in [XY+1, 2XY]$, which will not affect the image we need.

But, if we want to detect the vibration, the highest frequency we need becomes larger. The largest frequency is $f + (Xy_v + x_v - X)/T$, so the theoretical sample frequency and the frequency of the light pattern should also be increased to at least $2[f + (Xy_v + x_v - X)/T]$. However, the sample frequency does not need to reach the theoretical sample frequency; because the mirror signal of the vibration signal is quite weak, we only need to consider the mirror image of the stable object. The position of the mirror image of the stable object should be larger than that of the vibration signal with larger frequency.

In our experiment, the highest frequency of the light source is $XY/T = 1.78$ Hz, f = 210 min^{-1} = 3.5 Hz. When we set the frequency, the light pattern is increased to $4(XY/T) = 7.12$ Hz. The mirror image of the stable object that will appear at the position refers to 5.34–7.12 Hz, which will not affect the vibration detection, as shown in Fig. 4.

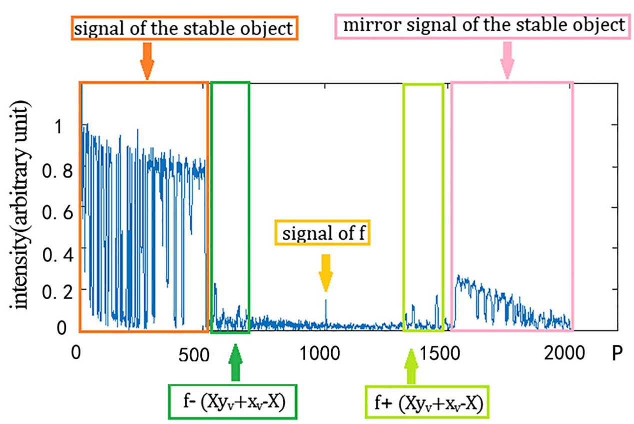

Fig. 4. Experiments of the vibration measurement with FMSI. The signals of the stable object and vibrating object, and mirror signal are shown.

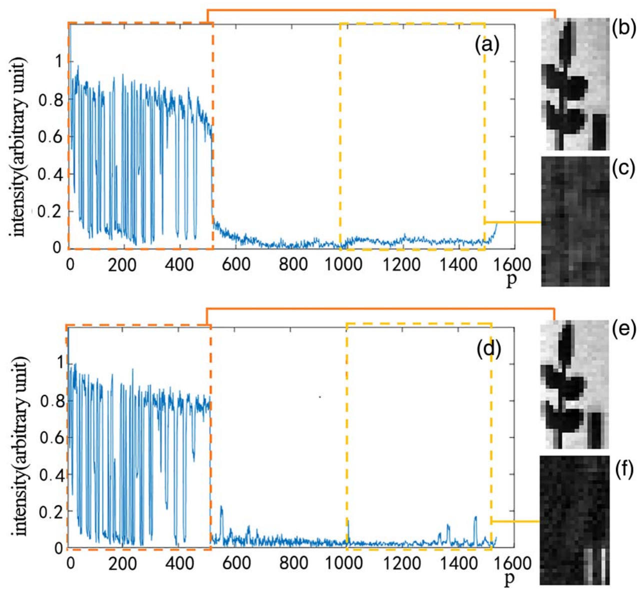

Fig. 5. Experiments of the vibration measurement with FMSI. (a) Fourier transformation of the signal when all the objects are stable, (b) single-pixel image when all the objects are stable, (c) single-pixel image of the same area as (f), (d) Fourier transformation of the signal when the cylinder is vibrating horizontally, (e) single-pixel image when the cylinder is vibrating horizontally, and (f) single-pixel image of the vibrating area.

As shown in Figs. 5(b) and 5(c), when all the objects are stable, FMSI can retrieve the image perfectly, and no vibration signal appears. When the cylinder is vibrating, the edge of the object will blur, as shown in Fig. 5(e), and the vibration signal and the signals of the edge of the object appear, as shown in Figs. 5(d) and 5(f).

The vibration signal appears at $p = 1008$, the measurement time $T = 287.3$ s, and we have $f = 210.5\ \mathrm{min}^{-1}$ due to Eq. (9), which is almost the same as the theoretical value of 210 min^{-1}.

What should be emphasized is that other orthogonal functions can also reconstruct the image, but that will be complex. With trigonometric function modulation, at the edge of the vibrating object, the intensity of transmitted light is transmittance multiplied by the intensity of light shining on that location. The signals with a difference and sum of their frequencies are produced. So, we can obtain the structure and vibration information of the object by a signal Fourier transformation, which is quite a simple process.

Also, as we use trigonometric function modulation, the signal of environmental light, especially the signal of electric light, may affect our result, for which their frequency is usually 50 Hz or its integer multiples. In this circumstance, we can remove these signals of particular frequencies in image processing or choose the appropriate frequency of the light source to avoid this disturbance.

5. Conclusion

We introduce a method to obtain vibration information with the FMSI method. This method uses a light source with a special pattern to illuminate the object, which can ensure that the light intensity signals at different positions have different frequencies. When the object has an in-plane vibration component, by analyzing the total light intensity signal transmitted or reflected by the sample, the position of the vibrating object and the vibration frequency can be obtained. By getting the vibration information, FMSI has the potential to finding the occurrence of abnormal conditions accompanied by unexpected vibration. Also, in addition to being able to measure vibration, FMSI has a similar SNR to other high-SNR single-pixel imaging methods[4].

Acknowledgement

This work was supported by the Nanjing University of Posts and Telecommunications (Nos. NY219148 and XK1060919148), Open Research Fund of the State Key Laboratory of Low-Dimensional Quantum Physics (No. KF202003), and Jiangsu Provincial Double-Innovation Doctor Program (No. CZ106SC20026).

References

1. T. Pittman, Y. Shih, D. Strekalov, and A Sergienko, "Optical imaging by means of two-photon quantum entanglement," Phys. Rev. A **52**, R3429 (1995).
2. H. Shapiro, "Computational ghost imaging," Phys. Rev. A **78**, 061802 (2008).
3. Z. Zhang, X. Ma, and J. Zhong, "Single-pixel imaging by means of Fourier spectrum acquisition," Nat. Commun. **6**, 6225 (2015).
4. R. Meyers, S. Deacon, and Y. Shih, "Ghost-imaging experiment by measuring reflected photons," Phys. Rev. A **77**, 041801 (2008).
5. G. Winters and R. Bartels, "Two-dimensional single-pixel imaging by cascaded orthogonal line spatial modulation," Opt. Lett. **40**, 2774 (2015).
6. F. Ferri, D. Magatti, L. A. Lugiato, and A. Gatti, "Differential ghost imaging," Phys. Rev. Lett. **104**, 253603 (2010).
7. W. Wang, Y. Wang, J. Li, X. Yang, and Y. Wu, "Iterative ghost imaging," Opt. Lett. **39**, 5150 (2014).
8. G. Li, Z. Yang, R. Yan, A. Zhang, L. Wu, S. Qu, and X. Zhang, "Iterative normalized correspondence ghost imaging," Optik **161**, 20 (2018).
9. W. Wang, X. Hu, J. Liu, S. Zhang, J. Suo, and G. Situ, "Gerchberg-Saxton-like ghost imaging," Opt. Express **23**, 28416 (2015).
10. M. Sun, M. Li, and L. Wu, "Nonlocal imaging of a reflective object using positive and negative correlations," App. Opt. **54**, 7494 (2015).
11. V. Katkovnik and J. Astola, "Compressive sensing computational ghost imaging," J. Opt. Soc. Am. A **29**, 1556 (2012).
12. O. Katza, Y. Bromberg, and Y. Silberberg, "Compressive ghost imaging," Appl. Phys. Lett. **95**, 131110 (2009).
13. Y. Xiao, L. Zhou, and W. Chen, "Fourier spectrum retrieval in single-pixel imaging," IEEE Photonics J. **11**, 7800411 (2019).
14. Y. Li, H. Yang, J. Liu, L. Gong, Y. Sheng, W. Cheng, and S. Zhao, "Colored object encoding scheme in ghost imaging system using orbital angular momentum," Chin. Opt. Lett. **11**, 021104 (2013).
15. D. Shi, S. Hu, and Y. Wang, "Polarimetric ghost imaging," Opt. Lett. **39**, 1231 (2014).